Approaching Micro-Arcsecond Resolution with VSOP-2: Astrophysics and Technology
ASP Conference Series, Vol. 402, © 2009
Y. Hagiwara, E. Fomalont, M. Tsuboi, and Y. Murata, eds.

Global Magnetohydrodynamic Simulations of Flares: Outflows and Time Variabilities in Black Hole Accretion Flows

R. Matsumoto

Department of Physics, Graduate School of Science, Chiba University, 1-33 Yayoi-Cho, Inage-ku, Chiba 263-8522, Japan

M. Machida

Division of Theoretical Astronomy, National Astronomical Observatory of Japan, 2-21-1 Osawa, Mitaka, Tokyo 181-8588, Japan

Abstract. We carried out global three-dimensional resistive magnetohydrodynamic simulations of radiatively inefficient black hole accretion flows. The disk magnetic fields, amplified by MRI, create magnetic loops emerging from the disk. Subsequently, these loops are twisted by the differential rotation of the disk and form large-scale poloidal magnetic fields even when the initial magnetic field is purely azimuthal. Semi-relativistic outflows emerge along the large-scale poloidal magnetic fields. By analyzing the simulation results, we obtained 43-GHz image of the launching region of outflows. We also discuss the possibility of detecting dynamo-driven reversals of mean magnetic fields.

1. Introduction

VSOP2 will reveal the structure of the jet launching region of accretion disks surrounding a super-massive black hole. Since the disk is optically thick at 43 GHz, the disk-corona interface will be mapped. This region is particularly important because magnetically-driven outflows emerge from this layer. Time dependent simulations of magnetically driven jets from accretion disks were carried out by Uchida & Shibata (1985) and Shibata & Uchida (1986), assuming axisymmetry and a disk initially threaded by large scale vertical magnetic fields. Hayashi, Shibata & Matsumoto (1996) showed that X-ray flares and outflows are produced when the magnetic loops connecting the central object and its disk are twisted by disk rotation. The inflating magnetic loops form a magnetic tower (Kato, Hayashi & Matsumoto 2004). Since the importance of the magneto-rotational instability (MRI) in accretion disks was pointed out by Balbus & Hawley (1991), nonlinear evolution of the MRIhas been studied by local 3D MHD simulations (e.g., Hawley et al. 1995) and by global 3D MHD simulations (e.g., Matsumoto 1999; Hawley 2000). We carried out global three-dimensional resistive MHD simulations of radiatively inefficient accretion disks inside 100 Schwarzschild radius from the black hole (Machida & Matsumoto 2003). In the following, we present the results of virtual observations of the simulation data at 43 GHz.

2. Formation of Black Hole Accretion Disks

Figure 1 shows results of global 3D resistive MHD simulations of the formation of black hole accretion disks. The initial state is an outer torus whose density maximum is at $\varpi = 35 r_\mathrm{s}$, where r_s is the Schwarzschild radius. The torus is embedded in spherical, low density, hot halo. General relativistic effects are simulated by using the pseudo-Newtonian potential $\phi = -GM/(r - r_\mathrm{s})$, where M is the black hole mass. We included Joule heating but neglected the radiative cooling. We assumed anomalous resistivity which sets in when J/ρ (J: current density, ρ matter density) exceeds a threshold. At the initial state, we assumed purely azimuthal weak magnetic field. The initial ratio of gas pressure to magnetic pressure $\beta = P_\mathrm{gas}/P_\mathrm{mag}$ at the density maximum is $\beta = 100$. The MHD equations expressed in cylindrical coordinates are solved by using the modified Lax-Wendroff scheme with artificial viscosity. The number of mesh points is $(N_\varpi, N_\varphi, N_z) = (250, 64, 398)$. We imposed absorbing boundary condition at $r = 2r_\mathrm{s}$. In the following, we use units $r_\mathrm{s} = c = 1$. The unit time is $\tau_0 = r_\mathrm{s}/c = 10^{-4} M/M_\odot$ sec.

The left panel of figure 1 shows the volume rendered image of the density distribution at $t = 60800$. The initial torus is deformed into an accretion disk. The mass accretion is driven by the angular momentum transport due to the Maxwell stress enhanced by the MRI-driven MHD turbulence.

The right panel of figure 1 shows the surface where the optical depth τ measured from top at 43 GHz is unity. The optical depth is computed by using the absorption coefficient of the synchrotron radiation. The power-law index of nonthermal electrons is assumed to be $p = 1$. The black hole mass and the initial maximum density of the torus are taken to be $M = 4 \times 10^6 M_\odot$ and $\rho_0 = 5.0 \times 10^{-15}$g/cm^3, respectively. At this frequency, the disk is optically thick. Spiral structures appear in the $\tau = 1$ surface.

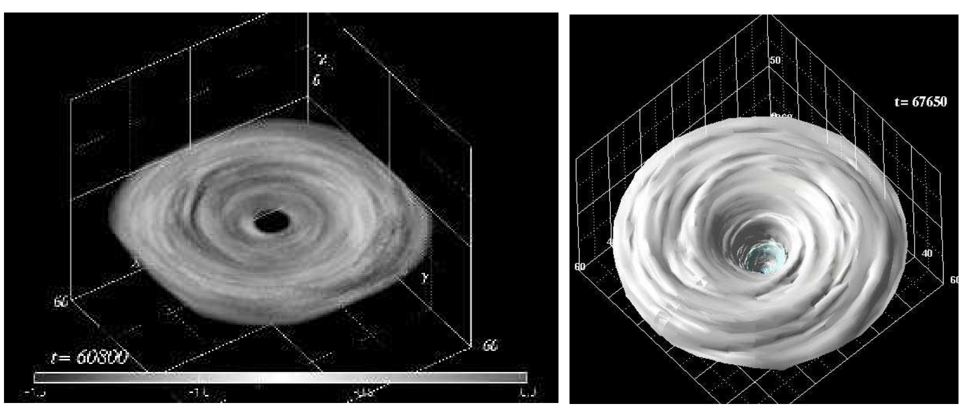

Figure 1. (Left) Volume rendered image of the density distribution. (Right) Isosurface where the optical depth is unity at 43 GHz when the disk is viewed from top.

3. Structure of the Jet Launching Region

Figure 2 shows the results of 3D global resistive MHD simulations starting from an initially hotter torus. The initial magnetic fields are purely azimuthal. We found that poloidal magnetic fields are generated in such disks. Solid curves in figure 2(a) show poloidal magnetic field lines. They become turbulent inside the disk due to the development of the MHD turbulence. In the funnel near the rotation axis, large-scale vertical magnetic fields are formed. Around the interface between the disk and the funnel, magnetic reconnections, taking place in the expanding magnetic loops, create outgoing plasmoids. These results are consistent with those of 2D MHD simulations by McKinney (2006) and 3D MHD results by Kato et al. (2004b) assuming initially poloidal magnetic fields embedded in the disk. We thus conclude that the final configuration of magnetic fields does not depend significantly on the initial condition.

Figure 2(b) shows the isosurface $v_{\rm z} = 0.05c$ (dark gray) and $\rho = 0.2\rho_0$ (light gray). Outflows emerge from the disk. The maximum speed of outflow is $v_{\rm z} \sim 0.1c$. The mass outflow rate increases with the disk temperature (Machida & Matsumoto 2008). The hot disk model presented here corresponds to the radiatively inefficient disk formed when the black hole candidate stays in the low/hard state. Numerical results are consistent with observations which indicate that sub-relativistic outflows exist in low/hard state (e.g., Fender & Belloni 2004).

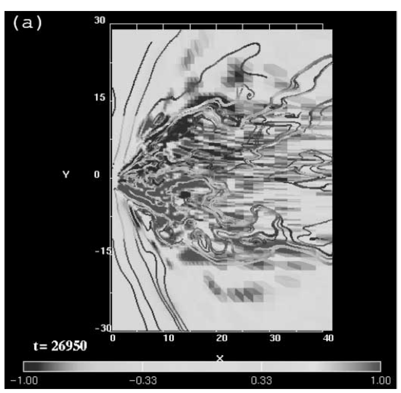

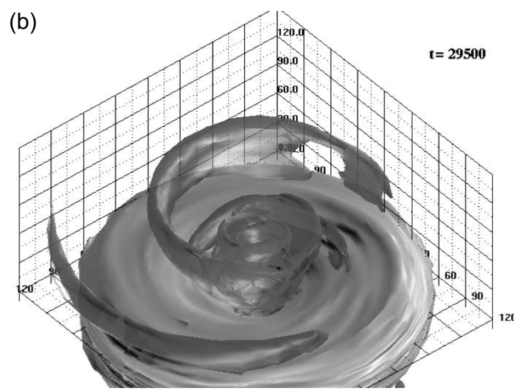

Figure 2. (a) Magnetic field lines projected onto the poloidal plane (solid curves) and distribution of azimuthal magnetic fields (gray scale). (b) Isosurface of $v_z = 0.05c$ (dark gray) and $\rho = 0.2\rho_0$ (light gray).

4. Reversal of Mean Magnetic Fields

Global 3D MHD simulations of rotating gas disks show reversals of mean azimuthal magnetic fields (Nishikori et al. 2006). The reversal is driven by the buoyant rise of magnetic flux from the disk to the disk halo. The typical time scale of field reversal is 10 rotation period. Figure 3 shows the mean azimuthal magnetic fields at $\tau = 1$ surface for frequencies 43 GHz, 230 GHz and 690 GHz at $\varpi = 10r_s$. The $\tau = 1$ surface is located deeper in the disk for higher frequency. At 43 GHz, we expect time variations of the polarization angle in time scale of $t \sim 0.2 - 1M/(10M_{\odot})$ sec, which corresponds to a few days in Sgr A*. This time variation manifests the dynamo cycle in accretion disks.

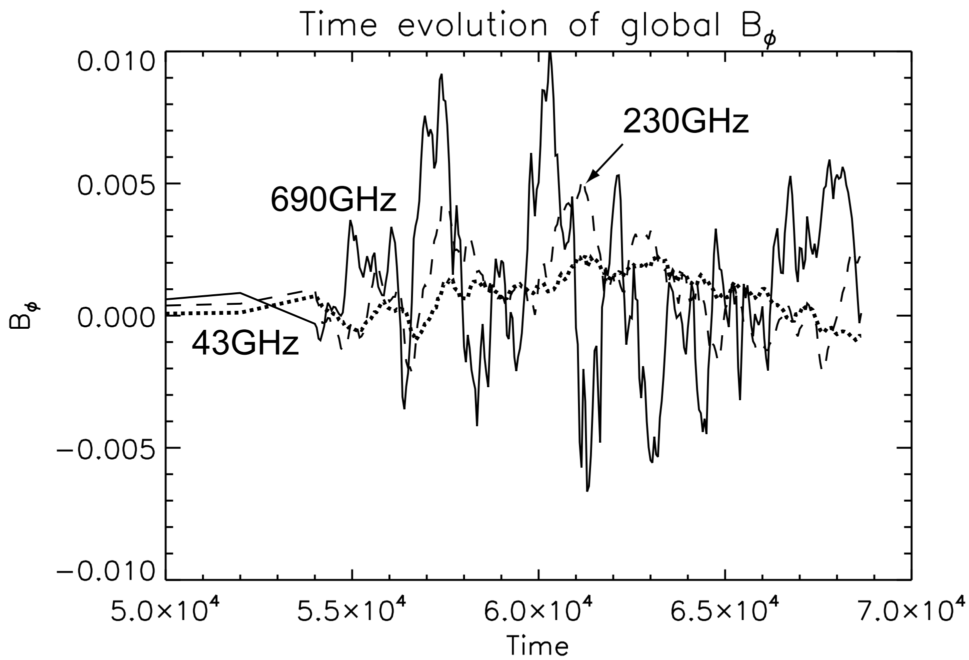

Figure 3. Mean azimuthal magnetic fields at $\varpi = 10r_s$ at $\tau = 1$ surface for 43GHz (dotted curve), 230GHz (dashed curve), and 690GHz (solid curve).

Acknowledgments. Numerical computations were performed by using VPP5000 at NAOJ. This work is supported in part by Grants-in-Aid for Scientific Research of MEXT, Japan (RM: 17030003).

References

Balbus, S. A., & Hawley, J. F., 1991, ApJ, 376, 214
Fender, R., & Belloni, T., 2004, ARA&A, 42, 317
Hawley, J. F., Gammie, C. F., & Balbus, S. A., 1995, ApJ, 440, 742
Hawley, J. F., 2000, ApJ, 528, 462
Hayashi, M. R., Shibata, K., & Matsumoto, R., 1996, ApJL, 468, 38
Kato, Y., Hayashi, M. R., & Matsumoto, R., 2004a, ApJ, 600, 338
Kato, Y., Mineshige, S., & Shibata, K., 2004b, ApJ, 605, 307
Machida, M., & Matsumoto, R., 2003, ApJ, 585, 429
Machida, M., & Matsumoto, R., 2008, PASJ in press (arXiv:0802.3779)
Matsumoto, R., 1999, in Numerical Astrophysics, Ed. S.M. Miyama, K. Tomisaka, & T. Hanawa, Kluwer, Boston, p.195
McKinney, J. C., 2006, MNRAS, 368, 1561
Nishikori, H., Machida, M., & Matsumoto, R., 2006, ApJ, 641, 862
Shibata, K., & Uchida, Y., 1986, PASJ, 38, 631
Uchida, Y., & Shibata, K., 1985, PASJ, 37, 515